

# $B_s^0 \rightarrow \mu^+ \mu^- \gamma$ without photon reconstruction: status and prospects at LHCb

Francesco Dettori<sup>1</sup>, Camille Normand<sup>2</sup> (they/them)

<sup>1</sup>Università degli Studi di Cagliari

<sup>2</sup>University of Bristol

29th February, 2024

Workshop on radiative  $B$  decays, Campus de Luminy (Marseille)



University of  
BRISTOL



Università degli Studi di Cagliari

INTENSITY

frontier



# Table of Contents

- 1  $B_s^0 \rightarrow \mu^+ \mu^- \gamma$  and the  $b$ -anomalies
  - $b \rightarrow s$  transitions
  - The  $B_s^0 \rightarrow \mu^+ \mu^- \gamma$  decay in the high- $q^2$  region
  
- 2 A search for  $B_s^0 \rightarrow \mu^+ \mu^- \gamma$  without photon reconstruction at LHCb

# Table of Contents

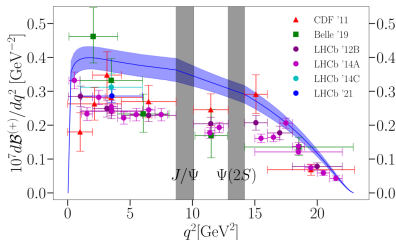
- 1  $B_s^0 \rightarrow \mu^+ \mu^- \gamma$  and the  $b$ -anomalies
  - $b \rightarrow s$  transitions
  - The  $B_s^0 \rightarrow \mu^+ \mu^- \gamma$  decay in the high- $q^2$  region
- 2 A search for  $B_s^0 \rightarrow \mu^+ \mu^- \gamma$  without photon reconstruction at LHCb

# “ $b \rightarrow s$ anomalies”

- The  $b \rightarrow s$  anomalies are a series of discrepant data described by a  $b \rightarrow s$  transition.
- Many observables give information on these transitions, with various ways to “dress” the quarks, and various decay properties:

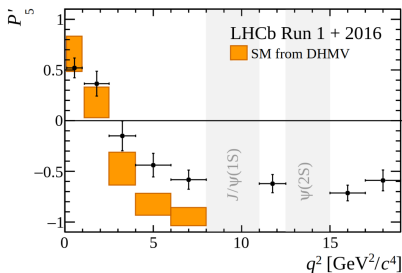
▶ Branching ratios (BR):  $\mathcal{B}(B \rightarrow K\mu\mu)$

[Parrott, Bouchard, Davies, Phys. Rev. D 107 (2023) 014510]



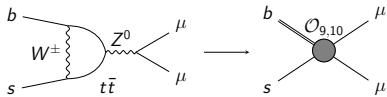
▶ Angular observables:  $P_5'$  ( $B \rightarrow K^*\mu\mu$ )

[LHCb collaboration, Phys. Rev. Lett. 125 (2020) 011802].

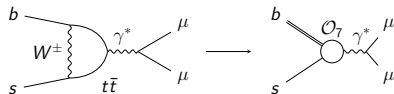


# Effective Theory of $b \rightarrow s$ decays

$$\mathcal{L}_{\text{eff}}^{b \rightarrow s \mu^+ \mu^-} = 2\sqrt{2}G_F \lambda^{\text{CKM}} \sum_i C_i^\mu \times \mathcal{O}_i$$

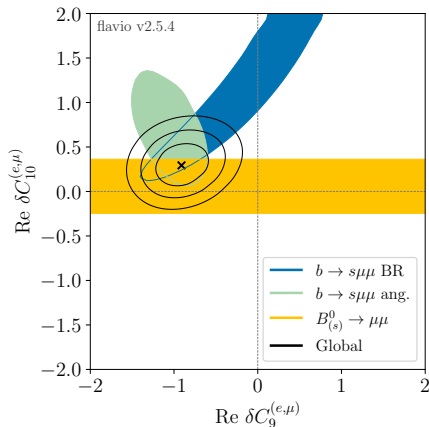


- Coupling strength of operator  $\mathcal{O}_i$  given by the **Wilson coefficient (WC)**  $C_i$ .



- $C_{7,9,10}^\mu$  are the WCs relevant to the loop-suppressed FCNCs.

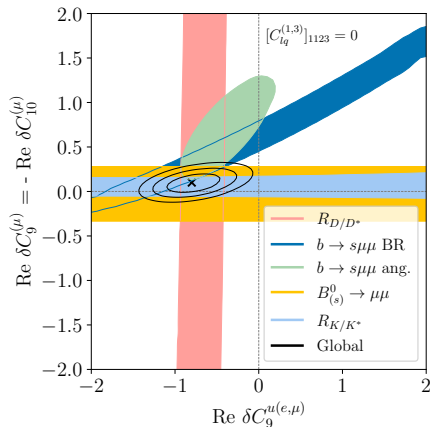
$$\delta C_9^\mu = \delta C_9^e \text{ vs. } \delta C_{10}^\mu = \delta C_{10}^e$$



- Equality between electronic and muonic Wilson coefficients removes the  $R_{K^{(*)}}$  constraints
- All subsets of data in agreement at the  $1\sigma$  level.
- $\mathcal{B}(B_s^0 \rightarrow \mu^+ \mu^-)$  gives  $C_{10}$  compatible with the SM at less than  $2\sigma$ .
- $C_9^\mu = C_9^e$  in tension with the SM !

[D. Guadagnoli, CN, S. Simula, L. Vittorio (2023), [JHEP 10 \(2023\) 102](#)]

# Connection with charged current anomalies



- Shift hinted at separately by  $b \rightarrow s$ - and  $b \rightarrow c$ -anomalies of the same order of magnitude.

[B. Bhattacharya, A. Datta, D. London, and S. Shivashankara (2014), [Phys. Lett. B, 742 \(2015\) 370-374](#)]

[D. Guadagnoli, CN, S. Simula, L. Vittorio (2023), [JHEP 10 \(2023\) 102](#)]

# The question

*“How do we confirm, or infirm, such a tension observed between predictions and measurements ?”*

✓ *“Are we observing New Physics ?”*

*or*

✗ *“A lack of knowledge of QCD ? (prediction)”*

*or*

✗ *“A mis-understanding of the data ? (measurement)”*



# The question

*“How do we confirm, or infirm, such a tension observed between predictions and measurements ?”*

✓ *“Are we observing New Physics ?”*

*or*

✗ *“A lack of knowledge of QCD ? (prediction)”*

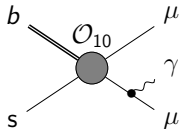
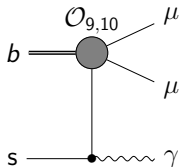
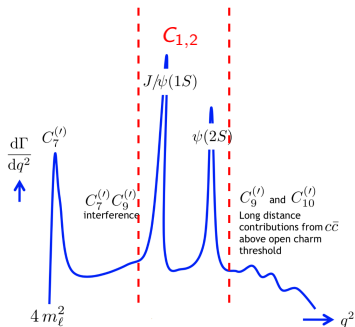
*or*

✗ *“A mis-understanding of the data ? (measurement)”*

$B_s^0 \rightarrow \mu^+ \mu^- \gamma$  in the high- $q^2$  region.

# The high- $q^2$ region

- $B \rightarrow V\mu\mu$  transition has a typical  $q^2 = m(\mu\mu)^2$  spectrum:



Initial and Final State Radiation

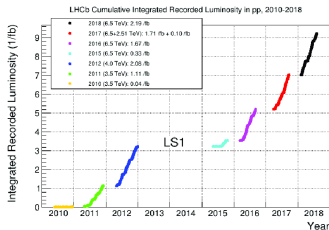
## The high- $q^2$ region

High- $q^2$  region  $\implies 4.2 \text{ GeV} < \sqrt{q^2} < m(B_s^0)$ , sensitive to  $C_9$  and  $C_{10}$ .  
 $\mathcal{B}(B_s^0 \rightarrow \mu^+ \mu^- \gamma)[4.2, m(B_s^0)] \text{ GeV} = (1.63 \pm 0.80) \times 10^{-10}$  in the SM.

# Table of Contents

- 1  $B_s^0 \rightarrow \mu^+ \mu^- \gamma$  and the  $b$ -anomalies
  - $b \rightarrow s$  transitions
  - The  $B_s^0 \rightarrow \mu^+ \mu^- \gamma$  decay in the high- $q^2$  region
- 2 A search for  $B_s^0 \rightarrow \mu^+ \mu^- \gamma$  without photon reconstruction at LHCb

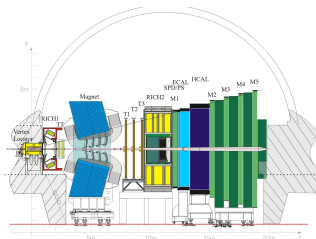
# The LHCb experiment



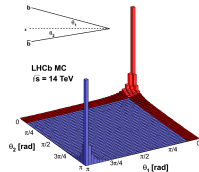
Integrated luminosity per year.

- Dedicated to  $b$ - and  $c$ -physics, here focus on proton-proton collisions.
- The amount of collected data, characterized by the **integrated luminosity**, totals  $9 \text{ fb}^{-1}$ .
- The collected data are divided into separate “runs”  
Run 1 in 2011-2012 and **Run 2 in 2015-2018**.

- Forward spectrometer:



The LHCb detector.

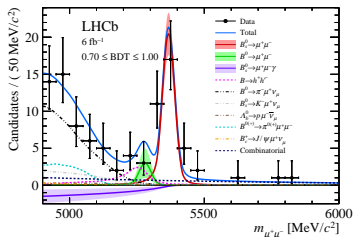


The  $b\bar{b}$  cross-section.

# From $B_s^0 \rightarrow \mu^+ \mu^-$ to $B_s^0 \rightarrow \mu^+ \mu^- \gamma$

- The latest measurement of  $B_s^0 \rightarrow \mu^+ \mu^-$  by LHCb shows that  $B_s^0 \rightarrow \mu^+ \mu^- \gamma$  can be accessed without reconstructing the (soft) photon

[LHCb collaboration, Phys. Rev. Lett. 125 (2020) 011802].



- Using only the di-muon information
  - ✓ increases the reconstruction efficiency
  - ✗ specializes the analysis to high- $q^2$
- Enlarging downward the mass region
  - ✓ increases the signal yield
  - ✗ increases the background yield

- The analysis is based on muon pairs with  $m(\mu^- \mu^+) \in [4.2, 6.0]$  GeV, and this requirement is understood throughout the talk.
- Current limit:  $\mathcal{B}(B_s^0 \rightarrow \mu^+ \mu^- \gamma) < 2.0 \times 10^{-9}$  with  $m(\mu^- \mu^+) < 4.9$  GeV.

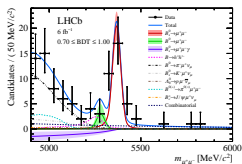
# Measuring $N(B_s^0 \rightarrow \mu^+ \mu^- \gamma)$

- The final expression reads

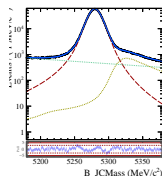
$$\mathcal{B}(B_s^0 \rightarrow \mu^+ \mu^- \gamma) = \frac{\mathcal{B}_{\text{norm.}}}{N_{\text{norm.}}} \times \frac{\epsilon_{\text{norm.}}}{\epsilon_{\text{sig.}}} \times \frac{f_d}{f_s} \times N(B_s^0 \rightarrow \mu^+ \mu^- \gamma)^{\text{obs.}} .$$

We choose two different normalisation channels,  $B^0 \rightarrow K^+ \pi^-$  and  $B^+ \rightarrow J/\psi K^+$ .

- $N(B_s^0 \rightarrow \mu^+ \mu^- \gamma)^{\text{obs.}}$  is extracted from a fit to the invariant di-muon mass similar to the  $B_s^0 \rightarrow \mu^+ \mu^-$  analysis



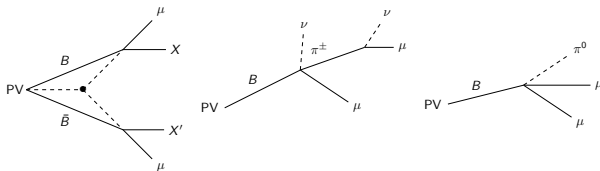
Normalization:



- Normalisation and signal efficiencies are determined on MC samples with inclusion of systematic uncertainties (ongoing).

# Backgrounds

- Several background sources:



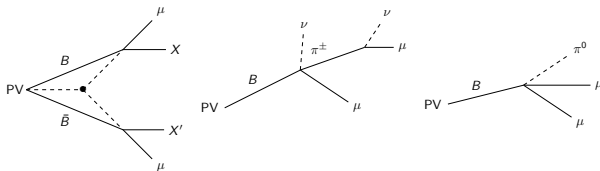
Combinatorial, mis-identified and signal-like backgrounds.

---

<sup>1</sup>apart from the combinatorial background

# Backgrounds

- Several background sources:



Combinatorial, mis-identified and signal-like backgrounds.

- Each background<sup>1</sup> comes with its efficiency,  $\epsilon_{\text{back.}}$ , computed individually.  
We want to minimize  $\epsilon_{\text{back.}}$ .

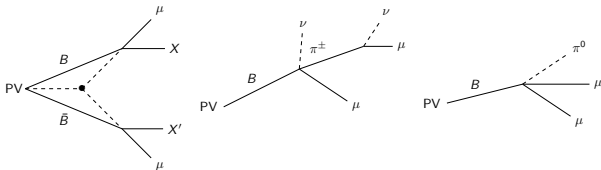
---

<sup>1</sup>apart from the combinatorial background



# Backgrounds

- Several background sources:



Combinatorial, mis-identified and signal-like backgrounds.

- Each background<sup>1</sup> comes with its efficiency,  $\epsilon_{\text{back.}}$ , computed individually.  
We want to minimize  $\epsilon_{\text{back.}}$ .
- Estimates for the number of background events:

$$\mathcal{B}(\text{back.}) = \frac{\mathcal{B}_{\text{norm.}}}{N_{\text{norm.}}} \times \frac{\epsilon_{\text{norm.}}}{\epsilon_{\text{back.}}} \times \frac{f_d}{f_i} \times N(\text{back.}) .$$

<sup>1</sup>apart from the combinatorial background

# Backgrounds

- Determine the **number of observed events** and **the efficiencies** for
  - ✓ the normalization channels (from the  $B_s^0 \rightarrow \mu^+ \mu^-$  analysis)
  - ✗ the signal channel
- For the backgrounds, the tasks are to
  - ▶ list the dominant backgrounds i.e. identify which processes could mimic our signal,
  - ▶ determine **the efficiencies**,
  - ▶ model the shape from MC samples,
  - ▶ estimate the number of **expected events (and the signal mass shape) from measured BRs.**

# Signal efficiency

$$\epsilon_{\text{tot}} = \epsilon^{\text{Acc}} \times \epsilon^{\text{Trig|Acc}} \times \epsilon^{\text{RecSel|Trig}} \times \epsilon^{\text{PID|RecSel}} \times \epsilon^{\text{BDT|PID}} .$$

- $\epsilon^{\text{Acc}} = (48.195 \pm 0.090)\%$

The decay products are in the acceptance of the detector.

- $\epsilon^{\text{Trig|Acc}} = (95.56 \pm 0.07)\%$

The decay products trigger the recording of the event.

- $\epsilon^{\text{RecSel|Trig}} = (6.25 \pm 0.21)\%$

Requirements to separate signal from backgrounds and “clean” the samples.

- $\epsilon^{\text{PID|RecSel}} = (92.76 \pm 0.09)\%$  vs  $(6.5 \pm 1.0)\%$  for  $\Lambda_b^0 \rightarrow p\mu^-\bar{\nu}_\mu$ .

Requirements dedicated to reducing mis-ID'd backgrounds.

- $\epsilon^{\text{BDT|PID}} \approx 30\%$

Multivariate Tool targeting combinatorial background.

---

$N_{\text{exp}}$	$2.41 \pm 1.21$
$N_{\text{exp}}[\mathcal{B}(m(\mu^+\mu^-) > 4.9 \text{ GeV}) = 2 \times 10^{-9}]$	$267 \pm 113$

---

# Boosted Decision Tree (BDT)

- Isolation variables, vertex fit quality, kinematic variables.

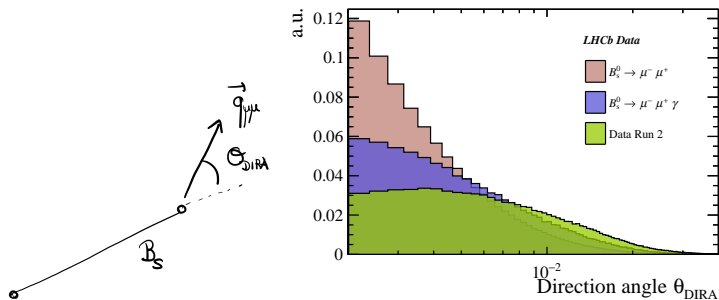


Figure: Distribution of the direction angle for  $B_s^0 \rightarrow \mu^+ \mu^- \gamma$  (signal),  $B_s^0 \rightarrow \mu^+ \mu^-$ , and data (combinatorial).

# $q^2$ -dependent efficiency

- The signal spans in  $q^2$ , such that the  $q^2$  dependency of the efficiency “shapes” the signal distribution.

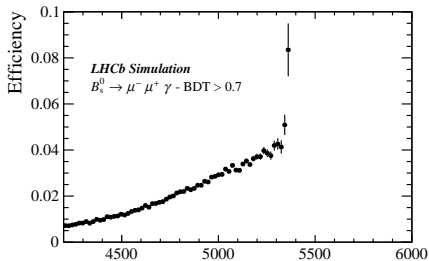
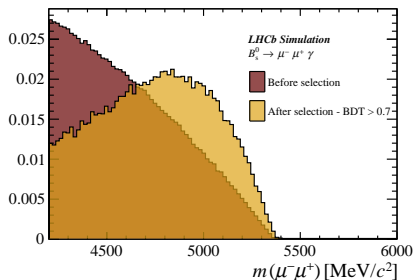
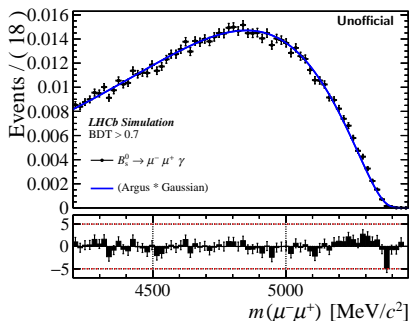


Figure: Di-muon invariant mass distribution of the signal (dark red) at the generation level and (light gold) after full selection containing a BDT requirement  $\text{BDT} > 0.7$ .

# Number of events and the signal mass shapes

- To fit the invariant mass distributions of the events, we need to **describe the shape of this distribution for the signal**.
- The signal mass distribution is determined from MonteCarlo (MC) simulations
- Represented by an Argus function convoluted with a Gaussian with a width fixed to the di-muon mass resolution from the  $B_s^0 \rightarrow \mu^+ \mu^-$  analysis at  $\sigma_{\text{res}} = 22.0 \text{ MeV}$



# Form factor parameterisation

- The choice of input form factor parameterisation influences the signal shape. (cf. Ludovico Vittorio's talk)

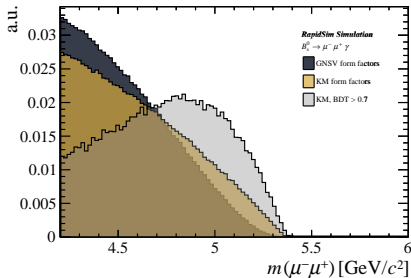


Figure: (Gold) KM parametrization and (black) the GNSV parametrization before selection.

- KM: [A. Kozachuk, D. Melikhov and N. Nikitin (2018), [Phys. Rev. D97 \(2018\) 053007](#)]
- GNSV: [D. Guadagnoli, CN, S. Simula, L. Vittorio (2023), [JHEP 07 \(2023\) 112](#)]

# Form factor parameterisation

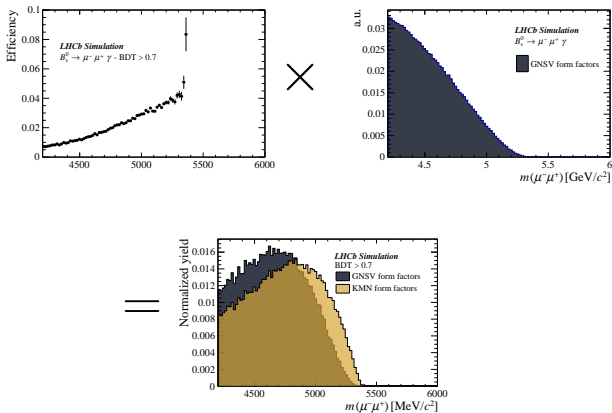


Figure: (Light) KM parametrization and (dark) the GNSV parametrization after selections.



# Invariant mass fit

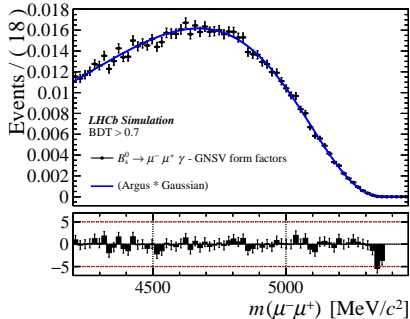
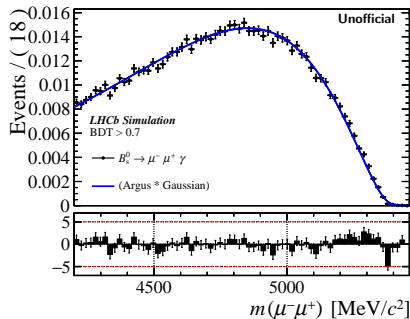


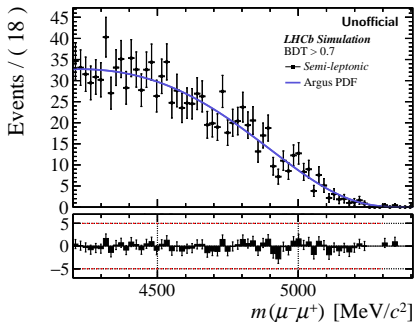
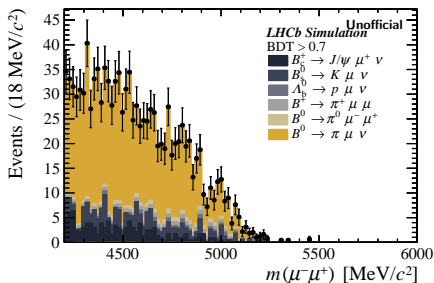
Figure: (Left) KM parameterisation and (right) GNSV parameterisation.

# Backgrounds - Semi-leptonic decays

- Semi-leptonic decays yields

Expected yield  $1136 \pm 158$

- Mass distribution



# Backgrounds - $B \rightarrow K\mu\mu$ decays

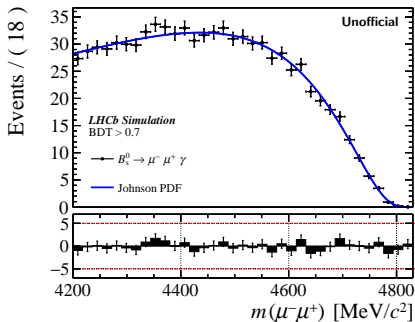
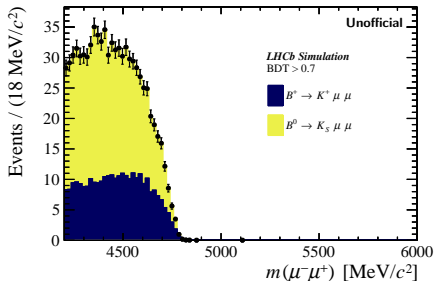
- $B \rightarrow P\mu\mu$  decays yields

---

Expected yield	$834 \pm 55$
----------------	--------------

---

- Mass distribution

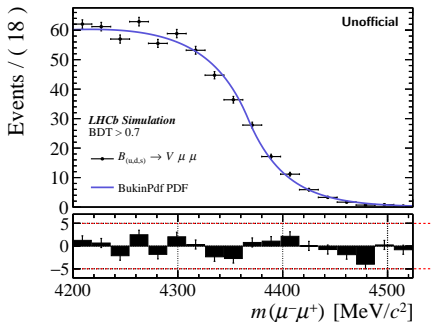
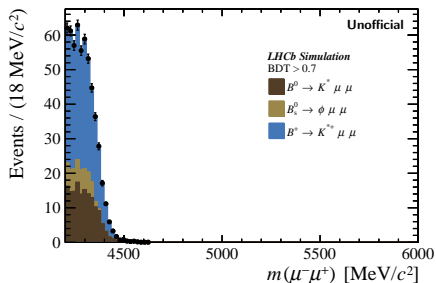


# Backgrounds - $B \rightarrow V\mu\mu$ decays, $V = K^*, \phi$

- $B \rightarrow V\mu\mu$  decays yields

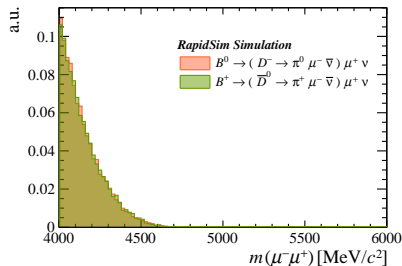
Expected yield	$562 \pm 32$
----------------	--------------

- Mass distribution

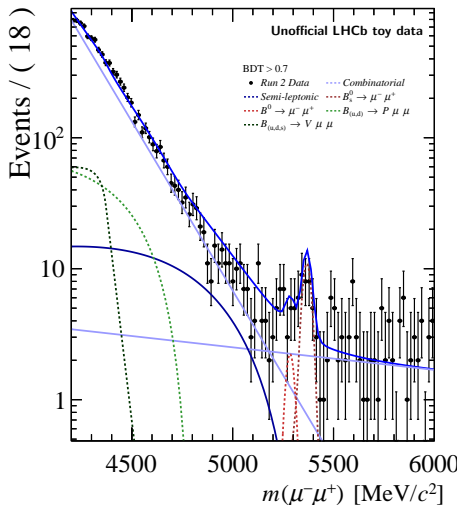


# Backgrounds - Combinatorial

- Unknown yield.
- Accounted for by a double-exponential PDF:
  - ▶ One for the combinatorial above the  $B_s^0$  mass;
  - ▶ One for partially-reconstructed “cascade decays”  $B \rightarrow (D \rightarrow \pi \mu \nu) \mu \nu$ .



# A first look at toy data



- 1 Background-only fit to the data i.e. no signal component to the fit (not shown).
- 2 Blinding: the number of expected event  $\sim 3$  means that the signal is not distinguishable in the data.  
→ Blinding is realized by not fitting for signal.
- 3 From this fit, we can extract the parameters for the combinatorial background.
- 4 All parameters and their uncertainties can be combined to generate toy data and compute the expected sensitivity of the analysis to the branching ratio of  $B_s^0 \rightarrow \mu^+ \mu^- \gamma$  (not shown).

# WIP and concluding remarks

- Including and constraining the cascade decays would allow for a **better control of the backgrounds** in the entire mass region, thus improving the upper-limit.
- Compute  $\epsilon_{\text{back.}}$  on **higher statistics MC**.
- Include systematic uncertainties: PID requirements, form factors parametrization.
- The partial reconstruction method proves to be useful to probe a **challenging phase-space of the decay**.

# Question time !

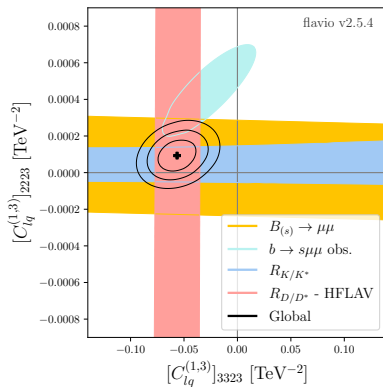
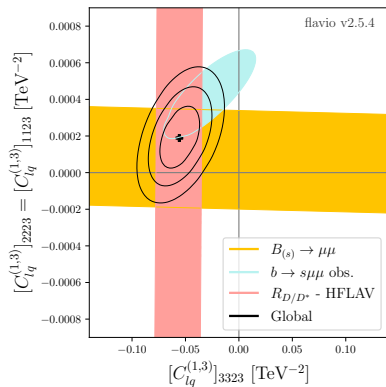
Thank you for your attention !

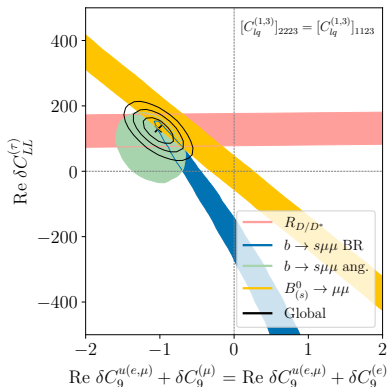
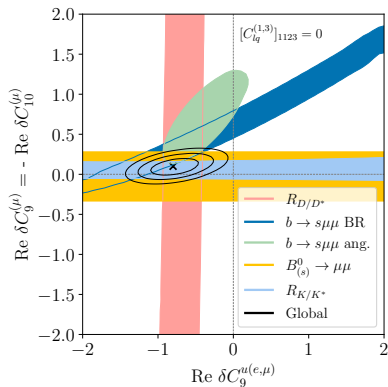


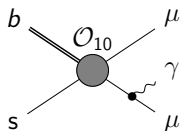
Back-up

# All scenarios

Scenario	Best-fit point	$1\sigma$ Interval	$\sqrt{\chi^{2,SM} - \chi^2}$
$(\delta C_9^{(\mu,e)}, \delta C_{10}^{(\mu,e)}) \in \mathbb{R}$	$(-0.88, +0.30)$	$([-1.08, -0.56], [0.15, 0.46])$	5.5
$\delta C_{LL}^{(\mu,e)}/2 \in \mathbb{C}$	$-0.70 - 1.36i$	$[-1.00, -0.54] + i[-1.77, -0.54]$	5.8
$\delta C_9^{(\mu,e)} \in \mathbb{C}$	$-1.08 + 0.10i$	$[-1.31, -0.85] + i[-0.70, +0.85]$	6.4
$\delta C_{10}^{(\mu,e)} \in \mathbb{C}$	$+0.68 + 1.40i$	$[+0.38, +1.00] + i[+0.69, +1.92]$	3.2
$\delta C_7 \in \mathbb{C}$	$+0.01 - 0.10i$	$[-0.015, 0.046] + i[-0.17, -0.05]$	2.6



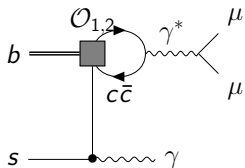




FSR component to the  $B_s^0 \rightarrow \mu^+ \mu^- \gamma$  amplitude

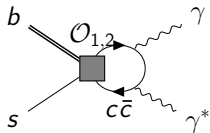
$$\bar{\mathcal{A}}_{\text{FSR}} = +i \frac{G_F}{\sqrt{2}} V_{tb} V_{ts}^* \frac{\alpha_{\text{em}}}{2\pi} e X_f f_{B_s} 2m_\mu C_{10} \times \left\{ \bar{u}(p_2) \left( \frac{\lambda^* \not{p}}{t - m_\mu^2} - \frac{\not{p} \lambda^*}{u - m_\mu^2} \right) v(p_1) \right\}, \quad (1)$$

# Long-distance contributions



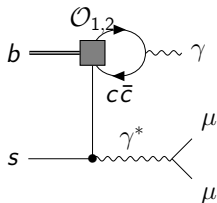
- Sum over  $\psi(3770)$ ,  $\psi(4040)$ ,  $\psi(4160)$ ,  $\psi(4415)$  of Breit-Wigner poles:

$$C_9^{\text{eff}}(q^2) \rightarrow C_9^{\text{eff}}(q^2) + \frac{9\pi \bar{C}}{\alpha_{\text{em}}^2} \sum_V |\eta_V| e^{i\delta_V} \frac{m_V \mathcal{B}(V \rightarrow \mu\mu) \Gamma_{\text{tot}}}{q^2 - m_V^2 + im_V \Gamma_{\text{tot}}}$$



- Power-suppressed at high- $q^2$

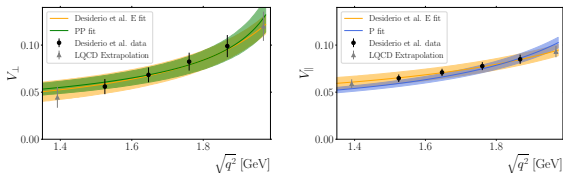
$$\bar{T}_\perp = T_\perp + \frac{16}{3} \frac{V_{ub} V_{ud}^* + V_{cb} V_{cd}^*}{V_{tb} V_{td}^*} \frac{a_1 f_{B_s^0}}{C_7^{\text{eff}} m_{B_s^0}}$$



- Power-suppressed at high- $q^2$

# $D_s \rightarrow \gamma$ form factors

- Direct Lattice computation of the form factors  $V_{\perp, \parallel}$  are available



- The Lattice data are well described by the following ansatz

$$V_{\perp}^{D_s}(q^2) = \frac{r_{\perp 1}^{D_s}}{1 - q^2/m_{D_s^*}^2} + \frac{r_{\perp 2}^{D_s}}{1 - q^2/m_{D_{s1}^*}^2},$$

$$V_{\parallel}^{D_s}(q^2) = \frac{r_{\parallel}^{D_s}}{1 - q^2/m_{D_{s1}^*}^2}.$$

- The  $D_{s(1)}^{(*)}$  are **physical states**:

- $D_s^*$  and  $D_{s1}^*$ :  $J^P = 1^-$
- $D_{s1}$ :  $J^P = 1^+$

# From $D_s \rightarrow \gamma$ to $B_s^0 \rightarrow \gamma$

- We use the following ansatz

$$V_{\perp}^{B_s}(q^2) = \frac{r_{\perp 1}^{B_s}}{1 - q^2/m_{B_s^*}^2} + \frac{r_{\perp 2}^{B_s}}{1 - q^2/m_{B_{s1}^*}^2},$$

$$V_{\parallel}^{B_s}(q^2) = \frac{r_{\parallel}^{B_s}}{1 - q^2/m_{B_{s1}}^2}.$$

with  $B_s^*$ ,  $B_{s1}^*$  and  $B_{s1}$  physical states of the  $B_s^0$  spectrum.



# From $D_s \rightarrow \gamma$ to $B_s^0 \rightarrow \gamma$

- We use the following ansatz

$$V_{\perp}^{B_s}(q^2) = \frac{r_{\perp 1}^{B_s}}{1 - q^2/m_{B_s^*}^2} + \frac{r_{\perp 2}^{B_s}}{1 - q^2/m_{B_{s1}^*}^2},$$

$$V_{\parallel}^{B_s}(q^2) = \frac{r_{\parallel}^{B_s}}{1 - q^2/m_{B_{s1}^*}^2}.$$

with  $B_s^*$ ,  $B_{s1}^*$  and  $B_{s1}$  physical states of the  $B_s^0$  spectrum.

- The **residues**  $r_i^{M_i}$  can be expressed

$$r_i^{M_i} = \frac{m_{M_i} f_{M_i}}{m_{M_i^*}} g_{M_i^* M_i \gamma}.$$

with the **tri-couplings**  $g_{M_i^* M_i \gamma}$  parameterize the coupling strength of  $M_i^* \rightarrow M_i \gamma$ .

# From $D_s \rightarrow \gamma$ to $B_s^0 \rightarrow \gamma$

- We use the following ansatz

$$V_{\perp}^{B_s}(q^2) = \frac{r_{\perp 1}^{B_s}}{1 - q^2/m_{B_s^*}^2} + \frac{r_{\perp 2}^{B_s}}{1 - q^2/m_{B_{s1}^*}^2},$$
$$V_{\parallel}^{B_s}(q^2) = \frac{r_{\parallel}^{B_s}}{1 - q^2/m_{B_{s1}^*}^2}.$$

with  $B_s^*$ ,  $B_{s1}^*$  and  $B_{s1}$  physical states of the  $B_s^0$  spectrum.

- The **residues**  $r_i^{M_i}$  can be expressed

$$r_i^{M_i} = \frac{m_{M_i} f_{M_i}}{m_{M_i^*}} g_{M_i^* M_i \gamma}.$$

with the **tri-couplings**  $g_{M_i^* M_i \gamma}$  parameterize the coupling strength of  $M_i^* \rightarrow M_i \gamma$ .

- The tri-couplings are parameterized in terms of **quark magnetic moments**, which follow a  $1/m_h$  scaling.  
↳ Using the LQCD data of the charm sector, we extract the tri-coupling and **extrapolate to the bottom sector**.

# Extrapolation to the bottom sector

- The form factors in the bottom sector thus require the determination of:
  - ▶ The mass  $m_{M_i}$ ;
  - ▶ The decay constant  $f_{M_i}$ ;
  - ▶ **The tri-coupling**  $g_{M_i^* M_i \gamma}$ ;of the excited states of the  $B_s^0$  with the relevant spin-parity.

- We parameterize the tri-couplings with a **heavy-quark expansion**

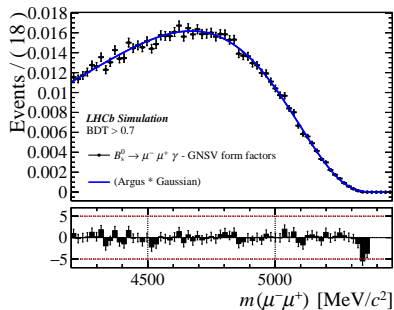
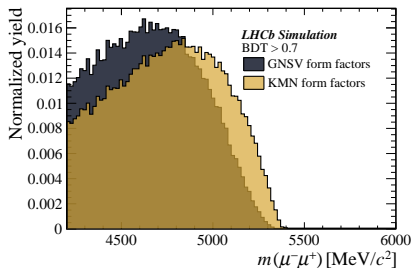
$$g_{D_{s1} D_s \gamma} = \mu_s^{\parallel} \left( -Q_s + Q_c \frac{m_s}{m_c} \right),$$

$$g_{B_{s1} B_s \gamma} = \mu_s^{\parallel} \left( -Q_s + Q_b \frac{m_s}{m_b} \right).$$

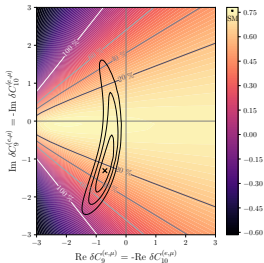
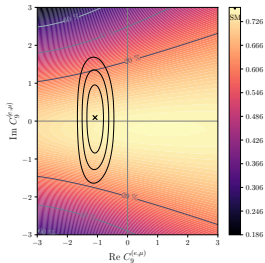
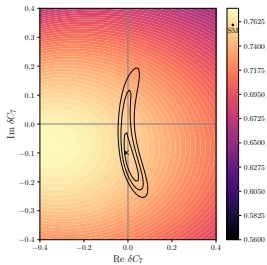
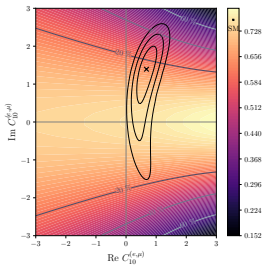
- From the LQCD form factors fit, we extract  $g_{D_{s1} D_s \gamma}$ , then  $\mu_s^{\parallel}$ , and finally  $g_{B_{s1} B_s \gamma}$ .

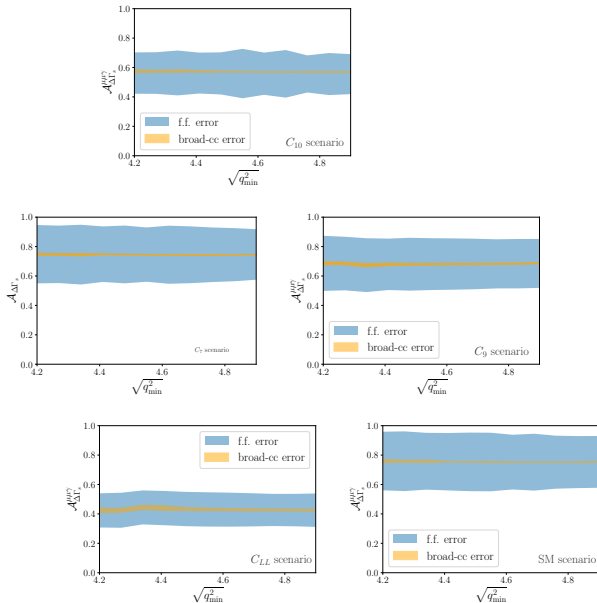
# Influence of the form factors parameterization

- The signal mass distribution of the MC depends on the form factors they are generated with

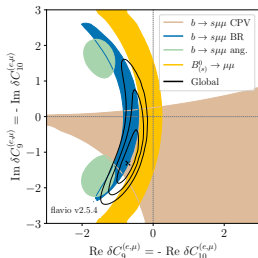
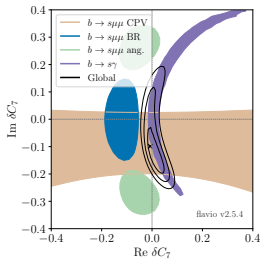
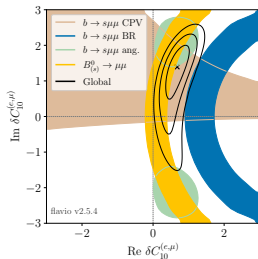
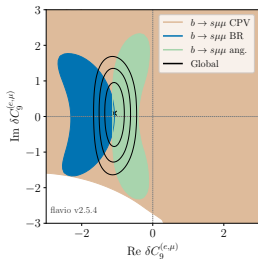


- It will be included as a systematic uncertainty.





# Complex fits



# Boosted Decision Tree (BDT)

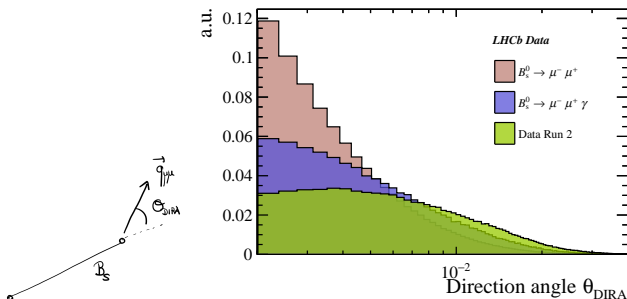


**Figure:** Distribution of the direction angle for  $B_s^0 \rightarrow \mu^+ \mu^- \gamma$  (signal),  $B_s^0 \rightarrow \mu^+ \mu^-$ , and data (combinatorial).